Activation of Diazene and the Nitrogenase Problem: An Investigation of Diazene-Bridged Fe(II) Centers with Sulfur Ligand Sphere. 2. Vibrational Properties

Nicolai Lehnert,[†] Beatrix E. Wiesler,[†] Felix Tuczek,*[,†] Andreas Hennige,[‡] and Dieter Sellmann[‡]

Contribution from the Institut für Anorganische Chemie und Analytische Chemie der Universität Mainz, Staudinger Weg 9, D-55099 Mainz, Germany, and Institut für Anorganische Chemie der Universität Erlangen-Nürnberg, Egerlandstrasse 1, D-91058 Erlangen, Germany

Received February 7, 1997[⊗]

Abstract: Resonance Raman and IR spectroscopic measurements of the two diazene-bridged systems [{Fe'N_HS_4'}$_2$-(N_2H_2)] ('N_HS_4'$^{2-}$ = 2,2′-bis(2-mercaptophenylthio)diethylamine(2−)) (I) and [{Fe'S_4'(PPr_3)}$_2$(N_2H_2)] ('S_4'$^{2-}$ = 1,2-bis(2-mercaptophenylthio)ethane(2−)) (II) including ^{2}H- and ^{15}N-isotopomers are combined with a normal coordinate analysis (NCA) in order to describe the vibrational properties of diazene coordinated to Fe(II)−sulfur centers. Eight of the 12 normal modes of the Fe-N_2H_2-Fe unit have been identified by their isotope shifts. Most of the Raman-active diazene vibrations are resonance enhanced with respect to the 600 nm transition providing further support to the assignment of this band as Fe(d) to diazene(π*) charge-transfer (MLCT) transition. The force constant for the N−N bond of 7.7 mdyn/Å corresponds to a N−N bond order of about 1.5 and indicates that the diazene unit is moderately activated. The force constant of the Fe−N bond of 1.8 mdyn/Å is about 2.5 times as large as for a simple σ-bond. These values confirm the σ-donor π-acceptor formulation of the Fe−diazene bond presented in part 1 of this paper. The splitting of the diazene N−H and N−D vibrations observed in the Raman spectra of II is ascribed to a photoisomerization process taking place upon irradiation into the MLCT band.

Introduction

In the preceding article a description of the electronic structure of two trans-μ-1,2 Fe(II)−diazene complexes, [{Fe'N_HS_4'}$_2$-(N_2H_2)] (I)[1] and [{Fe'S_4'(PPr_3)}$_2$(N_2H_2)] (II)[2] has been developed, based on Mössbauer and UV−vis spectroscopy coupled to SCF-Xα-SW calculations. The vibrational properties of these systems are the subject of the present paper. Early IR measurements of the diazene complex [{$Cr(CO)_5$}$_2$(N_2H_2)] including ^{2}H- and ^{15}N-substituted compounds have led to the identification of the symmetric and asymmetric N−X-stretching and N−X-bending vibrations (X = H, D) and the N−N stretch of the bridging diazene unit.[3] However, whereas a cis configuration of the diazene has been inferred from the spectroscopic data, the THF adduct [{$Cr(CO)_5$}$_2$(N_2H_2)]·2THF has been found to have a trans-μ-1,2 diazene bridge.[4] Attempts to obtain Raman data on a structurally characterized trans-μ-1,2 Ru−diazene complex analogous to II, [{Ru'S_4'(PPh_3)}$_2$(N_2H_2)], have been unsuccessful due to fluorescence and sample decomposition.[5] In order to determine the vibrational properties of the trans-μ-1,2 Fe(II)−diazene complexes I and II and to complement our electronic structure description, we have carried out low-temperature resonance Raman and FTIR measurements on these systems and the corresponding ^{15}N- and ^{2}H-isotopomers. Due to the inversion symmetry of the complex molecules, the information content of Raman and IR spectroscopy is complementary, and both spectroscopic methods are needed to obtain a complete set of vibrational frequencies. Most of the diazene vibrations are resonance enhanced with respect to the intense absorption band at 580 nm (I) and 620 nm (II), respectively, giving further support to our assignment of this band as metal-to-ligand charge-transfer (MLCT) transition. In combination with a normal coordinate analysis (NCA), these data lead to the first determination of the normal modes and force constants of complex-bound diazene. These are used for a comparison with free diazene the vibrational properties of which have been the subject of numerous investigations.[6]

Experimental and Computational Procedures

Sample Preparation, Isotopic Substitution. Complexes I and II with natural abundance isotopes were prepared as described before by (a) air oxidation of hydrazine precursors[1,2] or (b) directly by the azodicarboxylate method.[7] The ^{15}N-isotopomer of complex II has been prepared by method (a) using ^{15}N-hydrazinium sulfate (Cambridge Isotopes). The deuterium isotopomers of complexes I and II have been prepared by method (b) using CH_3COOD/D_2O as a deuterium source.

Raman Spectroscopy. Resonance Raman spectra were measured on a setup involving the following components: Spectra Physics 2020

* Corresponding author.
† Universität Mainz.
‡ Universität Erlangen-Nürnberg.
⊗ Abstract published in *Advance ACS Abstracts,* August 15, 1997.

(1) Sellmann, D.; Soglowek, W.; Knoch, F.; Moll, M. *Angew. Chem.* **1989**, *101*, 1244.
(2) Sellmann, D.; Friedrich, H.; Knoch, F.; Moll, M. *Z. Naturforsch.* **1994**, *48b*, 76.
(3) Sellmann, D.; Brandl, A.; Endell, R. *Angew. Chem., Int. Ed. Engl.* **1973**, *12*, 1019.
(4) Huttner, G.; Gartzke, W.; Allinger, K. *Angew. Chem., Int. Ed. Engl.* **1974**, *13*, 822.
(5) Sellmann, D.; Böhlen, E.; Waeber, M.; Huttner, G.; Zsolnai, L. *Angew. Chem.* **1985**, *97*, 984.
(6) (a) Carlotti, M.; Johns, J. W. C.; Trombetti, A. *Can. J. Phys.* **1974**, *52*, 340. (b) Bondybey, V. E.; Nibler, J. W. *J. Chem. Phys.* **1973**, *58*, 2125. (c) Nibler, J. W.; Bondybey, V. E. *J. Chem. Phys.* **1974**, *60*, 1307. (d) Frost, D. C.; Lee, S. T.; McDowell, C. A.; Westwood, N. P. C. *J. Chem. Phys.* **1976**, *64*, 4719. (e) Peric, M.; Buenker, R. J.; Peyerimhoff, S. D. *Can. J. Chem.* **1977**, *55*, 1533. (f) Peric, M.; Buenker, R. J.; Peyerimhoff, S. D. *Mol. Phys.* **1978**, *35*, 1495. (g) Craig, N. C.; Levin, I. W. *J. Chem. Phys.* **1979**, *71*, 400. (h) Hallin, K-E. J.; Johns, J. W. C.; Trombetti, A. *Can. J. Phys.* **1981**, *59*, 663. (i) Jensen, H. J. A.; Jørgensen, P.; Helgaker, T. *J. Am. Chem. Soc.* **1987**, *109*, 2895. (j) Fan, L.; Ziegler, T. *J. Chem. Phys.* **1990**, *92*, 3645. (k) Andzelm, J.; Sosa, C.; Eades, R. A. *J. Phys. Chem.* **1993**, *97*, 4664.
(7) Sellmann, D.; Hennige, A. *Angew. Chem.* **1997**, *109*, 270.

S0002-7863(97)00420-4 CCC: $14.00

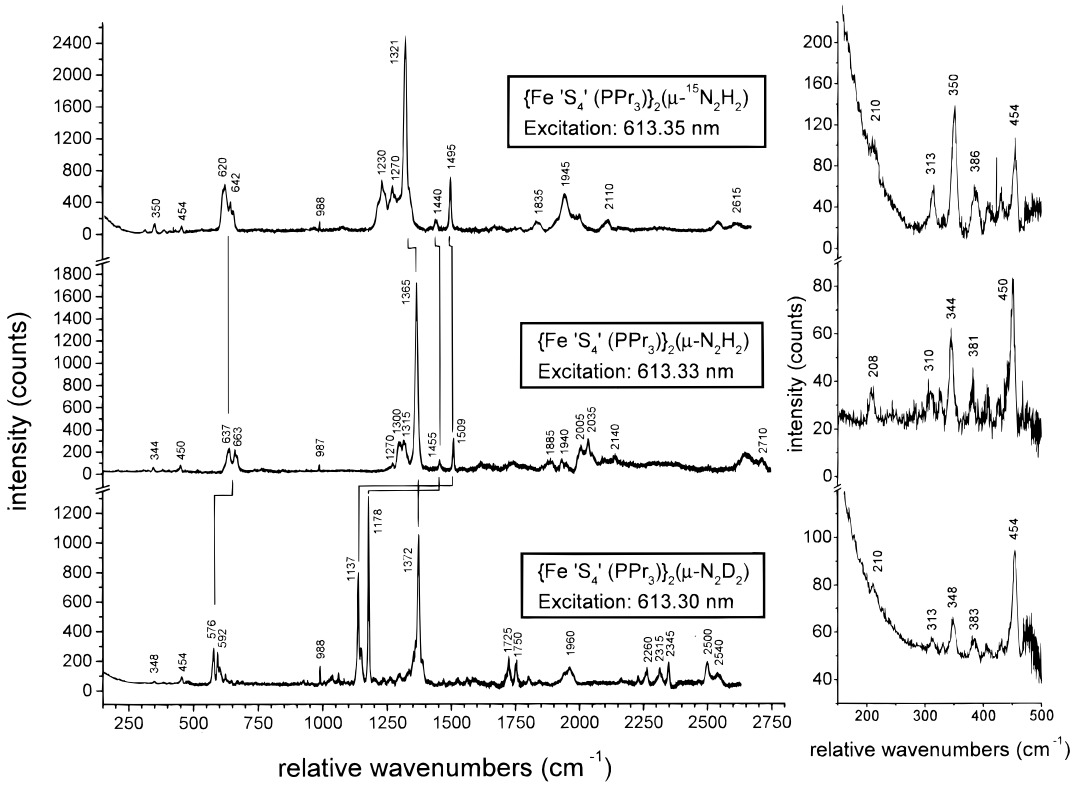

Figure 1. Resonance Raman spectra of complex II at 30 K. a) top: ^{15}N-substituted compound; b) middle: unlabeled complex; c) bottom: ^{2}H-substituted compound. All peak positions in cm^{-1}. The peaks at about 988 cm^{-1} belong to the A_1-breathing mode of K_2SO_4 added as an internal standard. Correlations between diazene vibrations in the different isotopomers are indicated.

5 W Ar^+-laser; Coherent 599 dye laser with rhodamine 6G; SPEX 1404 0.85 m double monochromator equipped with CCD camera (PI Instruments, 1024 × 256 pixels EEV chip) and Peltier-cooled RCA 31034 detector connected to a Stanford Research SR 400 photon counter allowing to record spectra in spectrograph or scanning mode; and liquid helium cryostat (Cryovac) for measurements from 4.2 to 300 K. Spectral bandpass was typically set at 4.5 cm^{-1}. Typical laser powers were 20 mW; the temperature was in general kept at 20−30 K. Higher laser powers or measuring temperatures were found to accelerate sample decomposition. Samples were ground and mixed 1:10 with K_2SO_4 as an internal standard and pressed into the groove of a copper holder placed into the stream of helium gas. All sample manipulations were performed in a glovebox.

IR Spectroscopy. MIR and FIR spectra were obtained on CsI pellets using a Bruker IFS 113 FTIR spectrometer equipped with a He cryostat. A DTGS detector has been employed both in the MIR and FIR region; light sources were a globar (MIR) or Hg-lamp (FIR). Typically, spectra were run at 10 K.

Normal Coordinate Analysis. Normal coordinate calculations were performed using the QCPE computer program 576 by M. R. Peterson and D. F. McIntosh which involves solution of the secular equation **GFL** = **ΛL** by the diagonalization procedure of Miyazawa.[8] The calculations are based on a general valence force field; force constants are refined with the nonlinear optimization routine of the simplex algorithm according to Nelder and Mead.[9] Since for a couple of normal modes no experimental frequencies have been available, the simplex optimization always has been used to refine only *selected* force constants. Normal eigenvectors were generated using the molecular graphics program XMole.[10]

Results and Analysis

A. Resonance Raman Measurements. The trans-μ-1,2 diazene bridged Fe-N_2H_2-Fe unit (symmetry C_{2h}) present in compounds I and II has 12 normal modes. These are the symmetric and antisymmetric in-plane Fe−N and N−H valence (ν) and deformation (δ) vibrations, respectively, the symmetric and antisymmetric out-of-plane (γ) vibrations, and the N−N stretch and the torsion around the N−N bond (τ). The six symmetric modes, i.e., ν_s(NH), ν_s(FeN), δ_s(NH), δ_s(FeN), γ_s, and ν(NN), are Raman active, whereas the six antisymmetric modes, ν_{as}(NH), ν_{as}(FeN), δ_{as}(NH), δ_{as}(FeN), γ_{as}, and τ, are IR active. In the following section we present the resonance Raman results obtained on compounds I and II.

Fundamental Vibrations of Compound II. The resonance Raman spectrum of the "S_4P" complex (compound II, Figure 1b) with excitation at 613 nm exhibits eight peaks below 2000 cm^{-1} at 637/663, 1270/1300/1315, 1365, and 1455/1509 cm^{-1} which shift in the spectra of the ^{2}H (Figure 1c) and ^{15}N (Figure 1a) isotope substituted compounds. The most intense peak at 1365 cm^{-1} shifts upon ^{15}N-substitution by 44 cm^{-1} and very litte upon deuteration and hence is assigned to the N−N stretch. In contrast, the pairs of peaks at 637/663 and 1455/1509 cm^{-1} exhibit a much larger shift upon deuteration than upon ^{15}N-substitution and thus are attributed to vibrations of primarily N−H character. Due to their relative energetic position, the peaks at 637/663 cm^{-1} (^{2}H-istope shift 61 and 71 cm^{-1}, respectively) correspond to the out-of-plane (γ_s) vibration which should be of mostly N−H type, and the peaks at 1455/1509 cm^{-1} (^{2}H-isotope shift 318 and 331 cm^{-1}, respectively) correspond to the N−H in-plane deformation. Raman excitation profiles have been recorded of the γ_s vibration at 637 and 663 cm^{-1}, of the 1365 cm^{-1} ν(NN)-stretching and of the 1509 cm^{-1} δ_s(NH)-bending mode (Figure 2). Clearly, all these vibrations are enhanced with respect to the electronic CT band at 620 nm. This is in accordance with their assignment as vibrations primarily involving the diazene unit and provides further support to the assignment of the 620 nm band as CT transition involving the diazene π^*_v orbital. The peaks at 1270, 1300, and 1315 cm^{-1} lying on the lower energy side of the N−N peak shift

(8) Miyazawa, T. *J. Chem. Phys.* **1958**, *29*, 246.
(9) Nelder, J. A.; Mead, R. *Computer J.* **1965**, *7*, 308.
(10) *XMole*, version 1.3.1; Minnesota Supercomputer Center, Inc.: Minneapolis, MN, 1993.

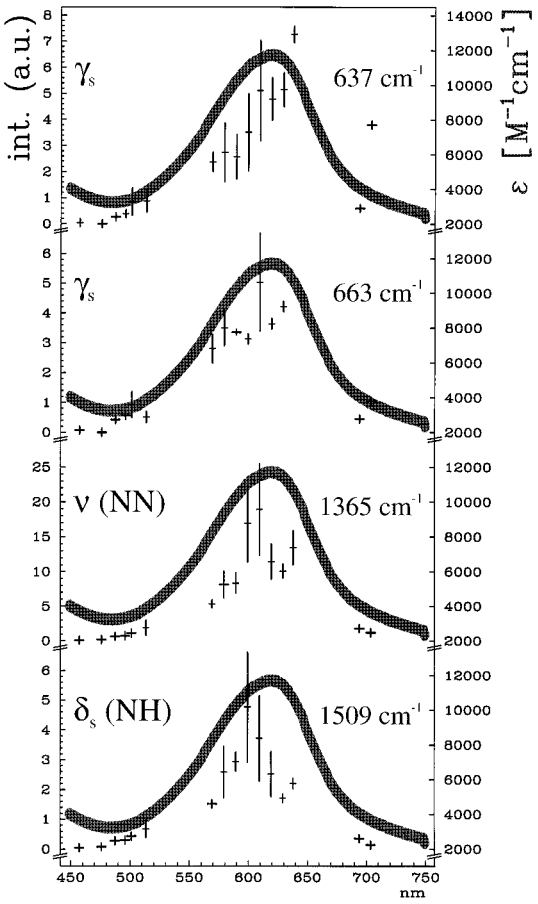

Figure 2. Resonance Raman excitation profiles of selected diazene modes of compound II along with the MLCT absorption band.

Table 1. Assignments of the Resonance Raman Spectra of *trans*-[{Fe'S_4'(PPr_3)}$_2$(N_2H_2)] (II) (in cm^{-1})

mode	symbol	N_2H_2	$^{15}N_2H_2$	N_2D_2
γ_s	A_1/A_2	637/663	620/642	576/592
ν(NN)	B	1365	1321	1372
δ_s(NH)	C_1/C_2	1455/1509	1440/1496	1137/1178
ν_s(NH)				(2230)/2315

Overtones and Combination Modes

	N_2H_2	$^{15}N_2H_2$	N_2D_2
$2 \times A_1/2 \times A_2$	1270/1300/1315	1230/1270	1150
$3 \times A_1/3 \times A_2$	1885/1940	1835	
$A_1 + B/A_2 + B$	2005/2035	1945	1960
$A_2 + C_1/A_1 + C_2$	2140	2110	1725/1750
$2 \times C_1/2 \times C_2$			2260/2345
$C_1 + B/C_2 + B$			2500/2540
$2 \times B$	2710	2615	

upon ^{15}N-substitution but are absent at this position in the spectrum of the deuterated complex. Hence they are assigned to overtones of the γ_s vibration (see below).

From about 1800 to 2700 cm^{-1}, there are additional peaks that change upon ^{15}N- and ^{2}H-isotope substitution, including a complex pattern around 2000 cm^{-1}. Most of these features can be assigned to combination modes (see below). In the region above 3000 cm^{-1} where the N−H stretch is expected and below 500 cm^{-1} where the ν_s(FeN) and δ_s(FeN) modes are anticipated to appear, only minor isotope shifts are observed which precludes a definitive assignment of these vibrations. The results are collected in Table 1.

Why do the δ_s(NH) and the γ_s vibrations which are of mostly N−H character split? A lowering of the effective symmetry cannot be the reason since both modes are nondegenerate. Rather, the very similar isotope shift of the two peaks assigned, e.g., to the γ_s vibration, their comparable shape, and the fact that no other diazene mode exists which could be responsible for an additional peak in that energetic region, strongly suggests that both peaks in fact belong to one identical mode; the same holds for the two peaks assigned to the δ_s(NH) vibration. This means that in the Raman sample (at least) two different species have to be present which differ in their vibrational properties. The possibility that the splittings are due to a phase transition of the matrix is excluded since they are observed in Raman spectra of solid solutions of II in CsI as well (data not shown). Another possible explanation would be that there are two different positions for the diazene protons at low temperature. However, the Raman spectra of the CsI samples also show the splittings at room temperature where only one hydrogen position has been determined from the X-ray structure.[2] On the other hand, splittings of N−H-bending vibrations have been found neither in the low- nor the room temperature IR spectra, and therefore the doubling of the γ_s and δ_s(NH) vibration peaks must be due to the laser irradiation.

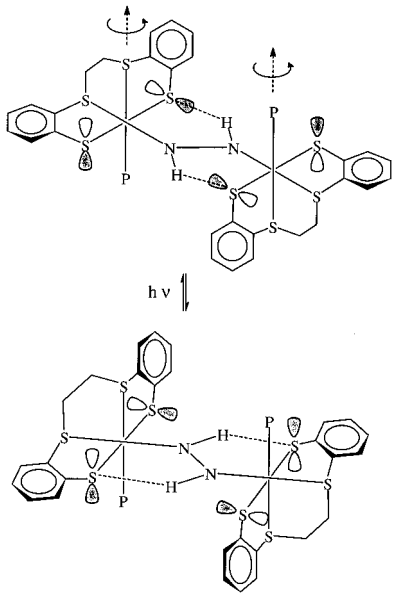

Figure 3. Diastereomers of compound II and proposed photoisomerization process (rotation around Fe−P axes). For complex I all thiolate lone pairs are in-plane (S−C(phenyl) bonds out-of-plane).

Hence, in order to explain the 15−30 cm^{-1} splitting of the γ_s and the 40−50 cm^{-1} splitting of the δ_s(NH) vibration, we are led to suggest that a photoisomerization takes place in the solid state upon laser irradiation. Since no time dependence of the Raman spectrum has been observed, the isomerization process must rapidly lead to a dynamical 1:1 equilibrium between two diastereomers. Sellmann et al. have demonstrated by NMR spectroscopy that by thermal isomerization of complex II in solution at around 0 °C a diastereomeric diazene complex is formed that is also centrosymmetric but features a different position of the N−H···S bridges.[2] This "hydrogen bridge diastereomerism" is due to the fact that in each Fe-'S_4' unit the two thiolate ligands lying cis in-plane to the bridging diazene group are nonequivalent (see Figure 3) since the S−C(phenyl) bond of one thiolate (S_{in}) lies within the diazene plane, but the S−C(phenyl) bond of the other thiolate ligand (S_{out}) is perpendicular to this plane. Correspondingly, the thiolate lone pair of S_{in} is perpendicular to the diazene-plane and the thiolate lone pair of S_{out} lies within it. In compound II, the S-Fe-N−N−H five-membered ring contains an S_{out} thiolate, and, hence, the thiolate lonepair is directed to the diazene H making a strong hydrogen bond. In the corresponding diastereomer, the five-membered ring contains a S_{in} thiolate and the lone pair is now perpendicular to the plane. Therefore the diazene hydrogens

are directed to the thiolate p-functions which bind the phenyl residues, and corresponding to the weaker donor capacity of these orbitals the resulting S···H bonds are weaker (cf. part 1 of this paper). In addition, diastereomers exhibit differing physical properties and thus probably also different mechanical couplings. Due to the hydrogen bridges, the bound thiolate donors will be displaced from their equilibrium positions during strong hydrogen movements. Therefore the N−H bend induces a S−C stretch in complex II but a S−C bend in the corresponding diastereomer. This could be a further reason for the large frequency difference of the N−H vibrations in both species. Evidently, the N−N stretch is unaffected by the photoisomerization as no splitting can be detected. This indicates that the binuclear Fe-N_2H_2-Fe core is retained and, moreover, that no photochemical loss of ligands (e.g., phosphine) takes place.

Closer examination of the two peaks of γ_s attributed to the two diastereomers shows that each peak is split again. This effect is pronounced in the ^{2}H-substituted compound (see Figure 1c) and further enhanced in the overtones of this mode (see below). We attribute these smaller splittings to strains and lattice defects around the complex molecules in the crystal lattice induced by the photoisomerization processes. Interestingly, this latter effect seems to be more important for the γ_s than for the δ_s(NH) vibration. One possible reason for this is that δ_s is a pure N−H bending mode, whereas γ_s has a contribution of out-of-plane Fe motion which may couple with a vibration of the out-of-plane iron ligands (thioether and phosphine). This way, the γ_s mode may be more sensitive to perturbations of the environment than the δ_s mode. We have tested these hypotheses by measuring a mixture of both diastereomers which has been prepared by rapidly stripping the solvent from a solution of complex II at room temperature (spectrum not shown). Again, the γ_s mode appears split by 31 cm^{-1}, however, slightly shifted (629/660 cm^{-1}), and broadened with respect to compound II. Whereas the broadening and the small shift show the influence of crystal quality on this mode, the important result lies in the fact that a physical mixture of both diastereomers basically gives the same Raman spectrum as pure compound II. In the IR-spectrum of the mixture, however, no splitting of δ_{as} at 1308 cm^{-1} could be detected (the other IR active modes are not sensitive enough to probe the structural changes). Eventually the δ_{as} band of the diastereomer is masked by other intense features in this spectral region.

A second remarkable feature of the spectra is the intensity increase of the N−D relative to the corresponding N−H peaks. This effect is particularly evident in case of the δ_s(NH) peak at 1455 cm^{-1} the intensity of which increases by a factor of 5 upon deuteration. While the intensity of the N−N stretch decreases, the second δ_s(ND) peak at 1178 cm^{-1} becomes even more intense than the N−N stretch which otherwise is the most intense peak of the spectrum at resonance conditions (Figure 1c). The same intensity increase can be observed for the N−H-stretching vibration: While no N−H stretch has been detected above 3000 cm^{-1} (see above), a peak at 2315 cm^{-1} appears in the spectrum of the deuterated compound which does not correspond to an overtone or combination mode (see below) and hence is assigned to the symmetric N−D stretch. The peak at 2230 cm^{-1} then probably is the second component of the N−D stretch which would correspond to the splitting of all other vibrations with N−H(D) contribution.

Comparison with Complex I. As expected, the Raman spectrum of compound I with the "N_HS_4" ligand system (excitation wavelength 613 nm) is very similar to that of compound II (Figure 4a). Thus, ν(NN) is found at 1382 cm^{-1}, γ_s at 667/659 cm^{-1}, and δ_s(NH) at 1480 cm^{-1}. However, δ_s is now unsplit and γ_s only split by 8 cm^{-1} ; in case of compound

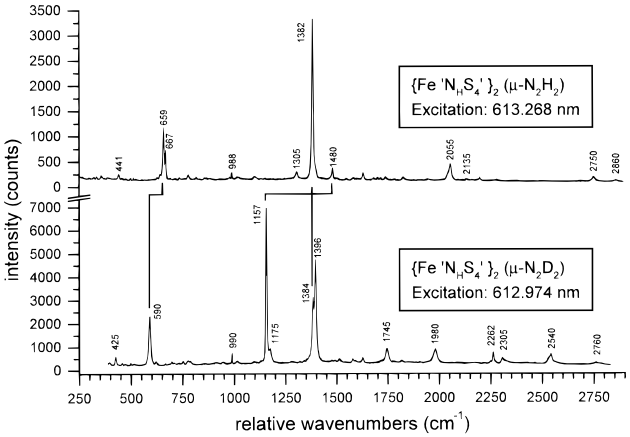

Figure 4. Resonance Raman spectra of complex I at 30 K. a) top: unlabeled complex; b) bottom: ^{2}H-substituted compound. All peak positions in cm^{-1}. The peaks at about 988 cm^{-1} belong to the A_1-breathing mode of K_2SO_4 added as an internal standard. Correlations between diazene vibrations in the different isotopomers are indicated.

Table 2. Assignments of the Resonance Raman Spectra of *trans*-[{Fe'N_HS'$_4$}$_2$ (N_2H_2)] (I) (in cm^{-1})

mode	symbol	N_2H_2	N_2D_2
γ_s	A	659/667	590
ν(NN)	B	1382	1384
δ_s(NH)	C	1480	1157
ν_s(NH)			2262

Overtones and Combination Modes

	N_2H_2	N_2D_2
2 × A	1305	1175
A + B	2055	1980
A + C	2135	1745
2 × C		2305
C + B	2860	2540
2 × B	2750	2760

II, this small splitting has been ascribed to inhomogeneities of the environment of the complex molecule induced by a photoisomerization processes. Since the 26 cm^{-1} splitting of γ_s and the 54 cm^{-1} splitting of δ_s(NH) observed in compound II are absent, we conclude that now both diastereomers exhibit very similar spectroscopic properties. This is compatible with our photoisomerization hypothesis as in case of compound I both S−C(phenyl) bonds of the in-plane thiolate ligands cis to the bridging diazene group are out-of-plane. Hence, the thiolate lone pairs are always within the diazene plane, and diazene is equivalently bound in the isomerization product and the parent complex. The small splitting observed for γ_s but not δ_s(NH) may be explained by the high sensitivity of the former mode for perturbations of the environment (see above) or by the fact that the isomerization product and the parent complex still are diastereomers. At 1305 cm^{-1}, the first overtone of γ_s appears. Above 2000 cm^{-1}, one observes exactly the same overtones and combination modes as in compound II (see Table 2).

Figure 4b displays the resonance Raman spectrum of the deuterated compound I. The γ_s peak at 590 cm^{-1} is not split but only slightly broadened. As in compound II, the bending mode δ_s(ND) appearing at 1157 cm^{-1} has enormously gained intensity such that it now becomes the most intense peak of the spectrum. The first overtone of γ_s is at 1175 cm^{-1}. Surprisingly, one now observes two intense peaks in the region of the N−N stretch. A plausible explanation for the appearance of a second band may be that deuteration of compound I with CH_3-COOD in D_2O also leads to partial exchange of the proton bound to the amine nitrogen of the 'N_HS_4' ligand. A further hint that this assumption is in fact true comes from IR spectroscopy:

Compound I shows an intense band at 3188 cm^{-1} that shifts upon ^2H-substitution to 2272 cm^{-1} (spectra not shown). The large intensity of this peak and the distinctly higher energy as compared with ν_{as}(NH) of II lead to the conclusion that this feature in fact belongs to the antisymmetric N−H stretch of the ligand amine groups. The frequency of the Raman peaks at 1384 or 1396 cm^{-1} would fit to a δ'(ND)-bending mode. Since the amine donors are trans to the diazene, this mode could in fact be resonance enhanced with respect to the Fe → diazene CT transition and thus become very intense. We assign the peak at 1384 cm^{-1} to the N−N stretch and the peak at 1396 cm^{-1} to δ'(ND) for the following reason: in the spectrum of the unlabeled compound I, an overtone of ν(NN) is observed at 2750 cm^{-1}, i.e., 14 cm^{-1} below the calculated value of 2764 cm^{-1}. At the corresponding position, i.e., $2 \times 1384\text{-}8 = 2760$ cm^{-1}, a peak is found in the spectrum of the deuterated compound which is therefore also assigned to the first overtone of the N−N stretch. Further support for this assignment is provided by the occurrence of the same combination modes with ν(NN) compared to the unlabeled complex. As in the deuterated complex II, a band appears around 2300 cm^{-1} which cannot be assigned to any overtone or combination mode. In analogy to compound II, the peak at 2262 cm^{-1} is assigned to the N−D stretch of the diazene group.

One additional feature appearing in the spectra of I compared with II is worth mentioning: Figure 4a shows a peak at 441 cm^{-1} that shifts upon deuteration to 425 cm^{-1}. Maybe this peak belongs to the mode ν_s(FeN) which should show a strong isotopic shift on deuteration (see normal coordinate analysis). However, we believe that this peak has to be assigned to the Fe−N stretch of the amine donor of the "N_HS_4" ligand, because the resonance Raman spectra of I and II are very similar with respect to the peak positions and their relative intensities. Therefore, if this peak belongs to ν_s(FeN) it should be observable in II as well.

Overtones and Combination Modes. Excitation into the maximum of the CT band leads to the enhancement of a number of overtones and combination modes: The three peaks at 1270, 1300, and 1315 cm^{-1} in the spectrum of compound II (Figure 1b) are assigned to the first overtone of γ_s at 637 and 663 cm^{-1} and not to a split peak of ν(NN), because they show a different behavior at ^2H-substitution than ν(NN) and therefore cannot belong to a splitting of this vibration. Moreover there is no additional Raman active fundamental of diazene in this energetic region which could be responsible for this observed features. Another argument for this assignment results from comparing both corresponding peaks in the spectrum of the ^{15}N-labeled compound at 1230/1270 cm^{-1} with the γ_s modes at 620/642 cm^{-1} (Figure 1a). Clearly both pairs of peaks have very similar shapes, but the relative intensities within the pairs have changed. This effect is even more pronounced in the spectrum of the unlabeled complex II (Figure 1b) where the first overtone of the 663 cm^{-1} fundamental is split into two peaks at 1300 and 1315 cm^{-1} : although the 637 and 663 cm^{-1} fundamentals are of almost equal intensity, the intensity of the first overtone of the 637 cm^{-1} vibration at 1270 cm^{-1} is much lower. An explanation for this observation in terms of the photoisomerization hypothesis (see above) may be that the 637 cm^{-1} peak is due to the diastereomer of compound II having a slightly different CT spectrum as compared to the original complex whence irradiation at 613 nm is slightly off-resonance. In general, the intensities of the first overtones of γ_s are equal to or higher than those of the fundamentals which is due to the fact that the overtones are totally symmetric in the C_{2h} point group of the Fe-N_2H_2-Fe unit and hence are subject to A-term resonance enhancement. In contrast, the fundamentals only have A_g symmetry in the C_i point group of the whole complex but not in C_{2h}, and therefore their A-term resonance enhancement is weaker. In case of the deuterated complex of II one overtone of γ_s(ND) can be identified at 1150 cm^{-1} which corresponds to the fundamental at 592 cm^{-1} shifted by 34 cm^{-1} to lower energy; the overtone of the other fundamental at 576 cm^{-1} may be hidden under the 1137 cm^{-1} peak. In complex I the first overtone of γ_s is observed at 1305 cm^{-1} shifting to 1175 cm^{-1} on deuteration. Altogether, the frequencies of the overtones are shifted by 10−20 cm^{-1} to lower energy due to anharmonicity effects and, in second order, to interaction with the N−N-stretch. Complex II shows further peaks at 1885 (calculated: 1911 cm^{-1}) and 1940 cm^{-1} (calculated: 1989 cm^{-1}), which are assigned to the third overtone of the γ_s vibration (^{15}N-isotopomer: 1835 cm^{-1}), showing that this vibration is in fact strongly anharmonic. First overtones of δ_s(ND) can also be observed (see Tables 1 and 2).

In addition the spectra show evidence for the excitation of a number of combination modes. Compound II shows a broad peak with two maxima at 2005 and 2035 cm^{-1} (Figure 1b) that is assigned to a combination mode of ν(NN) with the split γ_s vibration. Upon ^{15}N-substitution, this feature shifts below 2000 cm^{-1} showing an intense maximum at 1945 cm^{-1} with a broad shoulder centered around 2000 cm^{-1}. In the spectrum of the deuterated compound the γ_s modes lie closer together in energy, and therefore only one broad feature is observed at 1960 cm^{-1}, belonging to the combination of ν(NN) and γ_s. Interestingly the experimentally determined band positions lie somewhat above the calculated values which can be accounted for by positive vibrational coupling terms.[11] The same phenomenon is observed for compound I: the combination mode $\gamma_s + \nu$(NN) appears at 1980 cm^{-1} (calculated: 1974 cm^{-1}) in the ^2H-isotopomer and at 2055 cm^{-1} (calculated: 2041 cm^{-1}) in the unlabeled complex. Due to the large intensity of δ_s(ND) in the spectrum of the deuterated compound, combination bands between γ_s and δ_s(ND) can also be observed (see Tables 1 and 2).

B. IR Spectroscopy. Low-temperature IR spectra of compound II with the "S_4P" ligand system including ^{15}N- and ^2H-isotopomers have been measured in order to identify the antisymmetric vibrations of the Fe-N_2H_2-Fe moiety needed for normal coordinate analysis. Comparison of the three spectra displayed in Figure 5 leads to the determination of four modes.

In the middle-IR, two modes are observed that strongly shift upon deuterium substitution. Thus, the band at 1308 cm^{-1} (Figure 5b) shifts upon deuteration by 335 to 973 cm^{-1}. The energetic position of the band and the magnitude of the shift indicate that it must be the antisymmetric N−H-bending mode δ_{as}(NH). Note that the deuterium shift of the symmetric bend has been determined to 318/331 cm^{-1} (see section A). The additional peak at 956 cm^{-1} in the spectrum of the deuterated compound is ascribed to an impurity since there is no band other than at 1308 cm^{-1} missing up to 1600 cm^{-1}. The fact that the δ_{as}(NH) mode at 1308 and 1306 cm^{-1} (^{15}N-labeled compound), respectively, is unsplit in the IR spectra whereas a splitting of the corresponding symmetric δ_s(NH) mode is observed in the Raman measurements provides further evidence for the assumption that this splitting is due to the laser irradiation causing an isomerization of compound II. The other band showing an isotope shift is at 3130 cm^{-1}. It has very little intensity but is distinctly missing at this position in the spectrum of the deuterated compound. Instead, a new band appears at 2357 cm^{-1}. Since ν_s(ND) has been found at 2315/2230 cm^{-1}, we assign the band at 2357 cm^{-1} to ν_{as}(ND) and the band at 3130

(11) Wilson, E. B.; Decius, J. C.; Cross, P. C. *Molecular Vibrations*; McGraw-Hill: 1955.

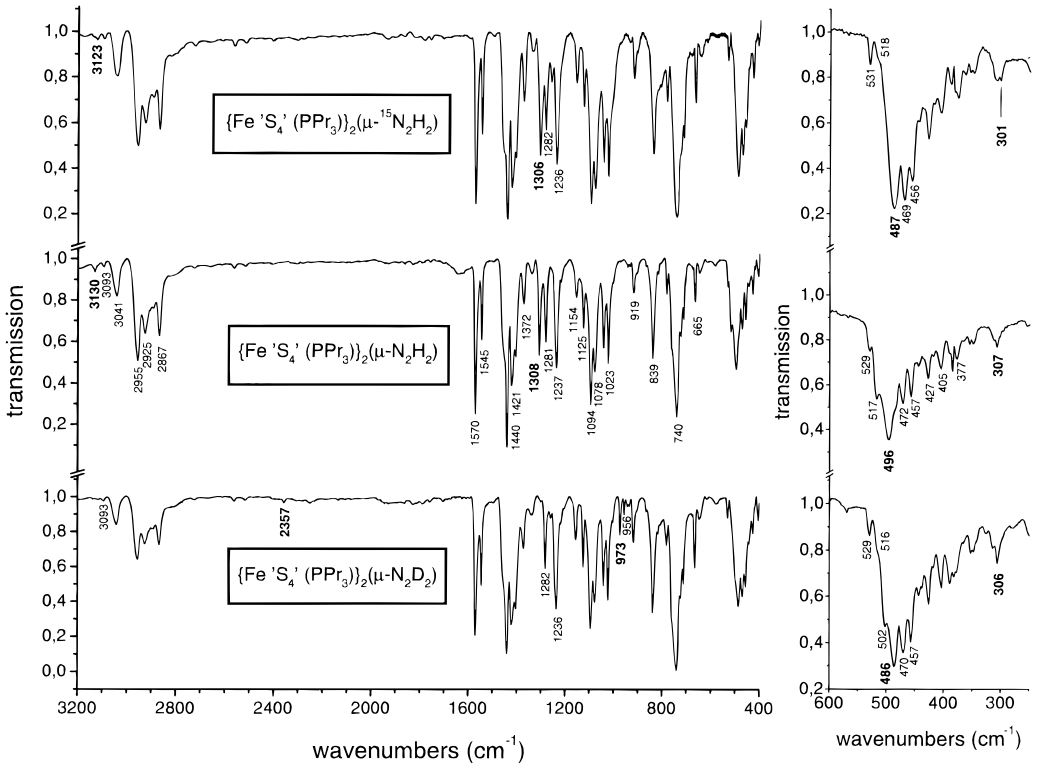

Figure 5. IR spectra of complex II at 10 K. a) top: ^{15}N-substituted compound; b) middle: unlabeled complex; c) bottom: ^{2}H-substituted compound. All peak positions in cm^{-1}. Band positions of diazene vibrations are given boldface.

Table 3. Assignments of the IR Spectra of *trans*-[{Fe'S$_4$'(PPr$_3$)}$_2$(N$_2$H$_2$)] (II) (in cm^{-1})

mode	N_2H_2	$^{15}N_2H_2$	N_2D_2
ν_{as}(NH)	3130	3123	2357
δ_{as}(NH)	1308	1306	973
γ_{as}			502 (?)
ν_{as}(FeN)	496	487	486
δ_{as}(FeN)	307	301	306

cm^{-1} to ν_{as}(NH), the symmetric counterpart of which could not be identified in the Raman spectra. Finally, there appears a band at 1259 cm^{-1} in the spectra of the ^{15}N- and ^{2}H-labeled compounds that is almost absent in the spectrum of the unlabeled compound II. We attribute this band to traces of stopcock grease.

In the far-IR region two modes appear that shift upon isotope substitution, i.e., at 496 cm^{-1} (^{15}N: 487 cm^{-1}, ^{2}H: 486 cm^{-1}) and at 307 cm^{-1} (^{15}N: 301 cm^{-1}, ^{2}H: 306 cm^{-1}). The former band is assigned to the antisymmetric Fe−N stretch ν_{as}(FeN) and the latter to the antisymmetric Fe−N bend δ_{as}(FeN). Unfortunately, the symmetric counterparts could not been identified in the Raman spectra. In addition, there appears a new band in the spectrum of the deuterated compound at 502 cm^{-1}. This could be the antisymmetric out-of-plane bend γ_{as}(ND) which possibly is masked in the other spectra by the intense absorption at 740 cm^{-1} (see section C and Table 4). It could also be due to an impurity, but this question cannot be decided with the present spectra. Table 3 contains the assignments.

Room-temperature IR data have also been obtained on compound I. The problem with this system is the partial deuteration of the amine nitrogen (see section A) which precludes unequivocal assignments based upon deuterium shifts. Hence, only IR data obtained from compound II are used for the normal coordinate analysis.

C. Normal Coordinate Analysis. Approach and Results. For the Fe(II)−diazene complex with the 'S$_4$'-phosphine ligand system (compound II) there exists a set of resonance Raman and IR spectra of the unlabeled as well as ^{15}N- and ^{2}H-isotope substituted compounds which allows for identification of most of the normal modes of the Fe-N$_2$H$_2$-Fe unit. These data are now used to carry out a normal coordinate analysis (NCA). The whole complex II has 378 vibrational degrees of freedom and is too large to be handled completely. In order to limit the number of force constants, the number of atoms included in the analysis has to be restricted. Figure 6 displays the central Fe-N$_2$H$_2$-Fe structure our NCA is based upon. Bond distances and angles have been adapted from the X-ray structure of II. Since most of the normal modes of complex II are internal vibrations of the 'S$_4$' and phosphine ligands which have little influence on the diazene vibrations, neglect of the peripheral ligand atoms is certainly justified. A more severe approximation is the neglect of the first sulfur/phosphine coordination sphere of the iron centers. This will in particular affect all vibrations involving significant Fe motion where strong coupling between Fe−N(diazene) and Fe−S or Fe−P metal−ligand vibrations may occur. In addition, the presence of N−H···S hydrogen bridges will influence all N−H vibrations and lead to discrepancies between the calculated and observed frequencies; these difficulties are considered in more detail below. Since the Fe-

Table 4. Comparison of the Observed and Calculated Frequencies of *trans*-[{Fe'S$_4$'(PPr$_3$)}$_2$(N$_2$H$_2$)] (II) (in cm^{-1})

	experimental			calculated		
mode	N_2H_2	$^{15}N_2H_2$	N_2D_2	N_2H_2	$^{15}N_2H_2$	N_2D_2
ν(NN)	1365	1321	1372	1365	1320	1373
ν_s(NH)			2315	3177	3171	2315
δ_s(NH)	1509	1496	1178	1509	1495	1177
γ_s	637	620	576	641	630	552
ν_s(FeN)				371	364	336
δ_s(FeN)				(170)	(169)	(165)
ν_{as}(NH)	3130	3123	2357	3138	3131	2294
δ_{as}(NH)	1308	1306	973	1310	1306	970
γ_{as}				763	761	555
ν_{as}(FeN)	496	487	486	499	487	481
δ_{as}(FeN)	307	301	306	(123)	(120)	(119)
τ				155	151	152

Table 5. Force Constants of the Internal Coordinates (***f***-Matrix) and Comparison with Empirical and SQM Force Fields of Free Diazene and Hydrazine for *trans*-[{Fe'S_4'(PPr_3)}$_2(N_2H_2)$] (II)

force constant[a]	symbol	complex I	free diazene N/B[c 6c]	free diazene C/L[c 6g]	free diazene J/J/H[d 6i]	free hydrazine C/S/F[c 13]
f_{r_1/r_1}	*X*	7.731	10.485	10.592	10.360	4.3
$f_{r_{13}/r_{13}}$	*Y*	5.539	5.370	5.418	5.424	6.1
$f_{r_{13}/r_{26}}$	*d*	0.113[b]	0.017	−0.027	−0.054	
$f_{\alpha_{13}/\alpha_{13}}$	*Q*	1.115	1.209	1.144	1.177	(0.79)
$f_{\alpha_{13}/\alpha_{26}}$	*g*	0.041	0.088	0.115	0.136	
$f_{r_1/r_{13}}$	*a*	0.310	−0.05	0	0.330	0.2
$f_{r_1/\alpha_{13}}$	r_1H	0.520	0.645	0.675	0.657	
$f_{r_{13}/\alpha_{13}}$	*rH*	0.373	0.375	0	0.094	
$f_{r_{13}/\alpha_{26}}$	rH_t	0.013	−0.362	0	0.095	
$f_{r_T/\tau}$	*T*	(0.4)	(0.5)	0.446	0.470	0.39
$f_{r_{14}/r_{14}}$	*Z*	1.823				
$f_{r_{14}/r_{25}}$	*e*	0.078				
$f_{\alpha_{14}/\alpha_{14}}$	*R*	0.330				
$f_{\alpha_{14}/\alpha_{25}}$	*h*	−0.08				
$f_{r_1/\alpha_{25}}$	*b*	−0.013				
$f_{r_1/\alpha_{14}}$	r_1Fe	0.044				
$f_{r_{14}/\alpha_{14}}$	*rFe*	0.195				
$f_{r_{14}/\alpha_{25}}$	rFe_t	0.015				
$f_{\alpha_{13}/\alpha_{14}}$	f_1	0.010				
$f_{\alpha_{13}/\alpha_25}$	f_2	−0.101				
f_{γ_1/γ_1}	*S*	0.184				
f_{γ_1/γ_2}	*i*	0.006				

[a] Units are mdyn/Å for stretching, mdyn·Å for bending and mdyn for stretch-bend interactions. [b] This force constant is overestimated, see NCA. [c] Empirical force field. [d] SQM force field.

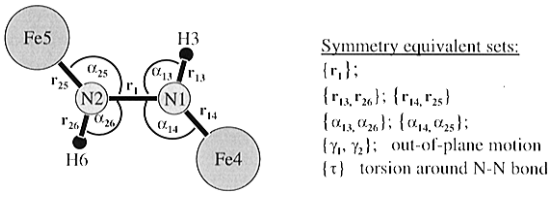

Figure 6. Central Fe-N_2H_2-Fe unit used for normal coordinate analysis. Definition of internal coordinates and symmetry equivalent sets.

N_2H_2-Fe structural unit is equally present in compound I with the 'N_HS_4' ligand, similar force constants should result by using the vibrational frequencies of this system. However, the information obtained on compound II is more complete (see section B), and the NCA is based only upon the frequencies of this complex. One problem associated with complex II is the presence of two diastereomers leading to band splittings in the Raman spectra; for the NCA, the frequency of the more intense peak has always been used (see Table 4).

The Fe-N_2H_2-Fe structural unit (symmetry C_{2h}) has 12 internal coordinates that can be divided into seven symmetry equivalent sets (see Figure 6). With the help of projection operators, symmetry coordinates are calculated. Scheme 1 displays the ***U***-matrix representing the transformation between internal and symmetry coordinates along with the irreducible representations of the latter. Scheme 2 contains the matrix of force constants for symmetry coordinates (***F***-matrix) in symbolic notation. One problem of the NCA lies in the fact that four vibrations have not been observed experimentally. Thus, ν_s(FeN) and δ_s(FeN) have not been found in the Raman spectra, but ν_{as}(FeN) and δ_{as}(FeN) have been identified in the IR spectra. Conversely, γ_{as} has not been observed in the IR spectrum, but γ_s has been identified in the Raman spectrum. Considering the ***F***-matrix (Scheme 2) it becomes apparent that the diagonal elements of the corresponding symmetric/antisymmetric modes are related by a nondiagonal element of the ***f***-matrix which should be small. The force constants of ν_s(FeN) and ν_{as}(FeN), e.g., are related by 2*e*. The force constant *e* of the ***f***-matrix relates the two internal coordinates r_{14} and r_{25} and certainly is an order of magnitude smaller than the diagonal element. Similar considerations apply for $\delta_{s/as}$(FeN) and $\gamma_{s/as}$(FeN). In these cases, the following stepwise procedure has been carried out: first, the diagonal force constant is adapted to the symmetric or antisymmetric mode with known frequency. This force constant is used in a first approximation in the other block of the ***F***-matrix containing the corresponding mode with unknown frequency which also provides a rough estimate of this frequency. Then the other force constants are varied in this block in order to reproduce the experimentally determined frequencies. Finally, all force constants are refined including the previously fixed diagonal force constant while allowing the frequency of the unobserved mode to vary within a certain margin around the approximate value. This way, reasonable frequencies and eigenvectors can be obtained for vibrations where one partner of a symmetric/antisymmetric pair is unobserved. The difference between the diagonal force constants of the symmetric and antisymmetric component also allows an estimate of the respective off-diagonal element in the ***f***-matrix (see above). This procedure only fails for the unknown torsion (τ) which is unobserved in the IR and has no symmetric partner. The corresponding force constant is assumed to be of the same magnitude as that of free diazene ($T = 0.4$)[6] and fixed in the NCA. This only serves to obtain an estimate of the frequency of this mode. The calculated force constants in terms of internal coordinates making up the ***f***-matrix are compiled in Table 5 (the corresponding ***F***-matrix can be generated by transforming ***f*** with ***U***); calculated and observed vibrational frequencies are given in Table 4.

Scheme 1. ***U***-Matrix Transposing Internal to Symmetry Coordinates

	r_1	r_{13}	r_{14}	r_{25}	r_{26}	α_{13}	α_{14}	α_{25}	α_{26}	γ_1	γ_2	τ
$A_g^{(1)}$	1	0	0	0	0	0	0	0	0	0	0	0
$A_g^{(2)}$	0	$\frac{1}{2}\sqrt{2}$	0	0	$\frac{1}{2}\sqrt{2}$	0	0	0	0	0	0	0
$A_g^{(3)}$	0	0	$\frac{1}{2}\sqrt{2}$	$\frac{1}{2}\sqrt{2}$	0	0	0	0	0	0	0	0
$A_g^{(4)}$	0	0	0	0	0	$\frac{1}{2}\sqrt{2}$	0	0	$\frac{1}{2}\sqrt{2}$	0	0	0
$A_g^{(5)}$	0	0	0	0	0	0	$\frac{1}{2}\sqrt{2}$	$\frac{1}{2}\sqrt{2}$	0	0	0	0
$B_g^{(1)}$	0	0	0	0	0	0	0	0	0	$\frac{1}{2}\sqrt{2}$	$-\frac{1}{2}\sqrt{2}$	0
$A_u^{(1)}$	0	0	0	0	0	0	0	0	0	$\frac{1}{2}\sqrt{2}$	$\frac{1}{2}\sqrt{2}$	0
$A_u^{(2)}$	0	0	0	0	0	0	0	0	0	0	0	1
$B_u^{(1)}$	0	$\frac{1}{2}\sqrt{2}$	0	0	$-\frac{1}{2}\sqrt{2}$	0	0	0	0	0	0	0
$B_u^{(2)}$	0	0	$\frac{1}{2}\sqrt{2}$	$-\frac{1}{2}\sqrt{2}$	0	0	0	0	0	0	0	0
$B_u^{(3)}$	0	0	0	0	0	$\frac{1}{2}\sqrt{2}$	0	0	$-\frac{1}{2}\sqrt{2}$	0	0	0
$B_u^{(4)}$	0	0	0	0	0	0	$\frac{1}{2}\sqrt{2}$	$-\frac{1}{2}\sqrt{2}$	0	0	0	0

Analysis. For the ν(NN), δ_s(NH), δ_{as}(NH), and ν_{as}(FeN) vibrations, very good agreement between calculated and observed frequencies was achieved demonstrating that the chosen model provides a useful basis to describe the diazene-centered vibrations. For the γ_s and $\nu_{s/as}$(NH) modes appreciable deviations from the experimentally determined values result. The origin of these discrepancies is most evident for γ_s which transforms in C_{2h} as B_g and thus cannot mix with any other mode of the Fe-N_2H_2-Fe unit. Hence, γ_s only has a diagonal force constant *S-i* (see ***F***-matrix) and no off-diagonal elements providing coupling with other modes. With this single force constant it is not possible to reproduce the observed frequencies of the three isotopomers (natural, ^{15}N, ^2H). In particular the frequency in the deuterated system is distinctly too low (552 vs 576 cm^{-1} observed). Obviously, the description of the out-of-plane vibrations within the chosen model is incomplete. This is related to the fact that γ_s contains an appreciable contribution of out-of-plane Fe motion. Since the iron atoms move relative to the out-of-plane ligands, mixing with the corresponding

Scheme 2. Symbolic ***F***-Matrix

$\nu_{N=N}$ $A_g^{(1)}$	ν_{NH} $A_g^{(2)}$	ν_{NFe} $A_g^{(3)}$	δ_{NH} $A_g^{(4)}$	δ_{NFe} $A_g^{(5)}$	γ $B_g^{(1)}$	γ $A_u^{(1)}$	τ $A_u^{(2)}$	ν_{NH} $B_u^{(1)}$	ν_{NFe} $B_u^{(2)}$	δ_{NH} $B_u^{(3)}$	δ_{NFe} $B_u^{(4)}$
X	$\sqrt{2}\,a$	$\sqrt{2}\,b$	$\sqrt{2}\,r_1H$	$\sqrt{2}\,r_1Fe$	0	0	0	0	0	0	0
$\sqrt{2}\,a$	$Y+d$	0	$rH+rH_t$	0	0	0	0	0	0	0	0
$\sqrt{2}\,b$	0	$Z+e$	0	$rFe+rFe_t$	0	0	0	0	0	0	0
$\sqrt{2}\,r_1H$	$rH+rH_t$	0	$Q+g$	f_1+f_2	0	0	0	0	0	0	0
$\sqrt{2}\,r_1Fe$	0	$rFe+rFe_t$	f_1+f_2	$R+h$	0	0	0	0	0	0	0
0	0	0	0	0	$S-i$	0	0	0	0	0	0
0	0	0	0	0	0	$S+i$	0	0	0	0	0
0	0	0	0	0	0	0	T	0	0	0	0
0	0	0	0	0	0	0	0	$Y-d$	0	$rH-rH_t$	0
0	0	0	0	0	0	0	0	0	$Z-e$	0	$rFe-rFe_t$
0	0	0	0	0	0	0	0	$rH-rH_t$	0	$Q-g$	f_1-f_2
0	0	0	0	0	0	0	0	0	$rFe-rFe_t$	f_1-f_2	$R-h$

metal−ligand vibration occurs which also is the reason for the sensitivity of γ_s to perturbations of the environment (see section A). This effect cannot be accounted for in the present model which does not include the out-of-plane sulfur and phosphine ligands. Much larger deviations are observed for δ_{as}(FeN), the frequency of which cannot even approximately be reproduced with the chosen model. Thus, the calculated frequency of δ_{as}(FeN) is 180 cm^{-1} lower than observed. This discrepancy can only be removed by using a four times larger diagonal force constant *R-h* which, however, corresponds to an unrealistic value. Probably, the calculated value for the symmetric bending mode δ_s(FeN) is equally more than 100 cm^{-1} too low as the corresponding diagonal element $R+h$ should approximately be as large as that of δ_{as} (see above). In this case, the neglect of the in-plane thiolate ligands is the origin for the difference between calculated and observed frequencies: Since the in-plane bending mode involves some Fe motion, the octahedral surroundings of the iron centers will not remain rigid which provides coupling with other in-plane metal−ligand vibrations. In fact, Fe-S stretching and bending modes are observed below 300 cm^{-1} [12] that may mix with the δ(FeN) modes and thereby shift their positions to higher energy. Certainly, δ(FeN) and γ are mostly affected by the limitations of the chosen model.

In contrast, the frequency of the Fe−N stretch ν_{as}(FeN) is reproduced very well. First, this may be due to the fact that the stretching movement causes the iron atom to oscillate nearly linearly between the nitrogen of diazene and the corresponding atom in trans position to it. Moreover, the high energetic position of ν_{as}(FeN) as compared with that of the bending modes leads to a smaller coupling with other low-lying metal−ligand vibrations.

Discrepancies between calculated and observed frequencies are also found for ν_{as}(NH). In particular, the calculated deuterium shift deviates from the observed value of about 770 by 60 cm^{-1} (ca. 10%). Unfortunately, ν_s(NH) only could be observed for the deuterated compound. For the calculation of the corresponding ν_s(NH) frequency, the diagonal force constant *Y-d* of ν_{as}(NH) was used as a first approximation, because the force fields of free diazene show that *d* should be small[6] and therefore the diagonal force constant $Y + d$ of ν_s(NH) should be very similar to *Y-d*. In the next step, this force constant was fitted to the observed value of ν_s(ND). Therefore, the force constant *Y-d* of ν_s(NH) is only derived from the frequency of the deuterated compound, whereas in the case of ν_{as}(NH) a fitting to all three frequencies was possible. Hence the difference of the diagonal force constants of both stretches is overestimated ($d = 0.1$) as compared to free diazene. Since the deuterium shift of ν_{as}(NH) was calculated 60 cm^{-1} too large, we suspect that a similar error occurs for the symmetric stretch and therefore the calculated values of 3177/3171 cm^{-1} (natural/^{15}N-isotopomer) probably are too high by at least 50 cm^{-1}. The problem of predicting wrong deuterium shifts for the N−H stretches with a harmonic force field has been noticed in the case of free diazene, too, and results from the strong anharmonicity of these modes.[6g] Moreover, we observe even stronger deviations, because our model complex neglects the strong hydrogen bridges of the diazene hydrogen atoms to the thiolate in-plane donors (see section A).

(12) *Infrared and Raman Spectra of Inorganic and Coordination Compounds*; Nakamoto, L.,Ed.; John Wiley: 1986.

Discussion

A. Frequencies and Force Constants. The Raman and IR spectroscopic measurements of compounds I and II have led to the first definition of the vibrational properties of complex-bound diazene. With the help of isotope frequency shifts, eight of the 12 normal modes of the trans-μ-1,2 Fe-N_2H_2-Fe unit could be observed; for three of the remaining vibrations, the other partner of the respective symmetric/antisymmetric pair has been observable such that an approximate estimate of the frequency of the "missing" mode could be obtained with the help of a normal coordinate analysis (NCA). The torsion mode has not been detected.

The diagonal force constants derived by the NCA are in general agreement with the σ-donor π-acceptor description of diazene presented in part 1 of this paper. The value of the N−N force constant in complex-bound diazene, $f_{r_1/r_1} = X = 7.73$, is intermediate between that of free diazene ($f_{r_1/r_1} = 10.485$)[6c] and hydrazine ($f_{r_1/r_1} = 4.3$;[13] all force constants in mdyn/Å). Applying the formula of Siebert,[14] the N−N-bond order in complex-bound diazene is 1.6. This position between a single and a double bond indicates that the weakening of the N−N bond caused by the π-acceptor function of diazene is more important than the strengthening of the N−N bond induced by σ-donation from the π^*_h orbital. This is due to the fact that π^*_h is primarily N−H bonding and to a weaker extent N−N antibonding, whereas π^*_v primarily is N−N antibonding. In the [{Cr(CO)$_5$}$_2$(N_2H_2)] complex,[3] the frequency of the N−N stretch (1415 cm^{-1}) is higher than in compound II (1365 cm^{-1}) probably because backbonding is weaker. This in turn is due to the presence of the backbonding CO coligands. The force constant of the N−H bond, $f_{r_{13}/r_{13}} = Y = 5.54$, is within the range of force constants determined for free diazene[6] but lies somewhat below that of hydrazine ($f_{NH} = 6.1$),[13] and ammonia ($f_{NH} = 6.54$).[15] This corresponds to the fact that the diazene protons are acidic and easily exchangeable but indicates that this acidity of diazene is not greatly altered upon complexation. Of further interest is a comparison between the Fe−N(diazene)

(13) Catalano, E.; Sanborn, R. H.; Frazer, J. W. *J. Chem. Phys.* **1963**, *38*, 2265.
(14) Siebert, H. *Z. Anorg. Allg. Chem.* **1953**, *273*, 170.
(15) Duncan, J. L.; Mills, I. M. *Spectrochim. Acta* **1964**, *20*, 523.

force constant $f_{r_{14}/r_{14}} = Z = 1.82$ and the known force constants for the M−N stretching modes in Co(II)− and Fe(II)− hexammine complexes.[16] For $[Fe^{II}(NH_3)_6]Cl_2$, e.g., the Fe−N valence mode frequencies are found between 300 and 350 cm^{-1} and the corresponding force constant is $f_{FeN} = 0.7 \pm 0.3$. These systems, however, have high-spin Fe(II) centers, while the diazene complexes are Fe(II) low-spin due to backbonding into the π^*_v orbital of diazene. This interaction strengthens the Fe−N bond and makes its force constant 2.5 times as large as for a pure Fe(II)−N σ-donor bond. In fact, the value of 1.82 gets close to the Co−N force constants in Co(III)−ammine complexes. In these systems which have Co(III) low-spin centers the Co−N valence modes lie in the range of 450−500 cm^{-1} corresponding to a force constant of $f_{CoN} = 1.86 \pm 0.6$. The low-spin configuration, however, is due to the higher charge of Co(III) as compared to Fe(II) and not to backbonding.

Large off-diagonal force constants are obtained in the NCA of complexes I and II for the coupling between the N−N stretch and the N−H stretch (element *a*) and, in particular, between the N−N stretch and the N−H bend (element r_1H). The latter interaction can be traced back to the competition between the N−N π-antibonding orbital π^*_h and the N−N σ-bonding orbital p_σ for bonding of the hydrogen atoms. If, e.g., the NNH-angle is increased from the equilibrium value, the overlap between 1s(H) and π^*_h becomes weaker and that between 1s(H) and p_σ larger. Hence, π^*_h becomes more strongly N−N antibonding and p_σ less strongly N−N bonding. Consequently, the N−N equilibrium distance increases and the N−H bend and the N−N stretch become coupled.[17] Similar overlap considerations explain the smaller but still relatively large stretch−stretch interaction (element *a*) and the stretch−bend interactions as expressed by the matrix elements *rH* (N−H bond) and *rFe* (Fe−N bond). In contrast, all off-diagonal matrix elements between internal coordinates of a symmetry equivalent set (*d*, *e*, *g*, *h*, *i*) are small, as expected. Only *d* is somewhat larger ($d = 0.11$) which is related to the way the ν(NH) force constants have been determined (see NCA).

B. Raman Enhancements and Nature of the Excited State. The assignment of the 580 and 620 nm bands of complexes I and II to $d_{yz}-\pi_v \rightarrow \pi_v^*-d_{yz}$ CT transitions can now be employed to interpret the resonance Raman data. Since the orbital π^*_v is N−N antibonding, a change of the N−N equilibrium distance between ground and excited state is expected, and all modes that involve motion along the N−N bond should be A-term resonance enhanced. This primarily applies to the N−N stretch which in fact shows strong enhancement with respect to the MLCT transition. However, the N−H-bending and γ modes are significantly enhanced, too (see Figure 2). The A-term resonance enhancement of these vibrations is not immediately understandable since the π^*_v orbital is perpendicular to the diazene plane and therefore has no contribution from the hydrogen atoms. Hence, no displacement along the N−H-stretching and bending coordinates should occur upon a transition from the ground to the MLCT excited state. This consideration, however, neglects two effects: (1) N−N-stretching and N−H-bending motions are mixed as determined by our normal coordinate analysis (see above), and (2) the enlargement of the N−N bond distance associated with the MLCT transition may entail some increase of the NNH-angle and eventually some elongation of the N−H bond in the excited state. The last effect may be very small as the π^*_h to π^*_v transition of free diazene shows no progression in the N−H vibration, and, hence, no displacement of the N−H coordinate is observed even if one electron is transferred from an orbital that is N−H bonding.[18] This may also explain the absence of any detectable N−H stretch intensity in the Raman spectra. The increase of the NNH-angle due to the MLCT transition is related to the ground state coupling mechanism between N−N stretch and N−H bend described above.

For a quantitative determination of the resonance enhancements of the different normal modes, a normal coordinate analysis would have to be carried out both for the ground and the excited state, and Franck−Condon factors between ground and excited state vibrational wave functions would have to be calculated.[19] For a qualitative discussion, the excited state displacement is expanded according to

$$\Delta Q = \sum_{i=1}^{3N-6} a_i \cdot Q_i = \sum_{i=1}^{3N-6} \Delta Q_i \qquad (1)$$

where the sum runs over all ground state normal modes. We assume that the relative enhancement of a particular mode *i* is given by the square of ΔQ_i, in analogy to treatments involving only one active vibration.[20] For simplicity, it is further assumed that the excited-state distortion ΔQ primarily consists of an elongation of the N-N bond (i.e., effect (2) is neglected; see above). In the $N_2{}^1H_2$ compound, ΔQ is then mostly described by ν(NN) (Figure 7) representing a pure N−N motion. Note that the hydrogen atoms almost follow the motion of the nitrogen atoms. The fact that the arrows on hydrogen are somewhat smaller than those on nitrogen corresponds to a (small) admixture of N−H-bending motion in ν(NN). Hence, a small contribution of the in-plane bending mode δ_s(NH) has to be added to correctly describe ΔQ which according to (1) leads to a displacement in this mode as well and thus to its resonance enhancement. In the N−N stretch of the deuterated compound, on the other hand, the deuterium atoms barely follow the motion of the nitrogen atoms (see Figure 7) and, hence, this mode has a much larger contribution of N−D-bending motion. Therefore, at least one contribution of δ_s(ND) has to be added in order to describe the excited-state displacement in (1). This contribution, however, is much larger than in the ^{1}H-isotopomer case which explains the large increase of the δ_s(ND) as compared to the δ_s(NH) peak intensity observed upon excitation at the maximum of the MLCT band. On the other hand, the ν(NN) contribution in the expansion (1) now is smaller than in the $N_2{}^1H_2$ case, and hence ν(NN) is less enhanced in the deuterated compound than in the unlabeled complex (see Figures 1 and 2). Thus, the higher extent of mode mixing in the deuterated as compared to the ^{1}H compound is reflected in a more symmetric distribution of A-term Raman intensity.

In analogy to the dependence of the in-plane NNH-angle upon the in-plane electron distribution (see above), population of the π^*_v orbital perpendicular to the diazene-plane should lead to some out-of-plane movement of the hydrogen atoms. This may explain the Raman resonance enhancement of the γ mode with respect to the 580 and 620 nm MLCT transition, respectively. Note that this vibration is due to bonding of the diazene unit to the iron centers and is absent in free diazene. In addition to the displacements considered so far, i.e., elongation of the N−N

(16) (a) Schmidt, K. H.; Müller, A. *Coord. Chem. Rev.* **1976**, *19*, 41. (b) Hitchman, M. A. *Inorg. Chem.* **1982**, *21*, 821.

(17) Wong, D. P.; Fink, W. H.; Allen, L. C. *J. Chem. Phys.* **1970**, *52*, 6291.

(18) (a) Back, R. A.; Willis, C.; Ramsay, D. A. *Can. J. Chem.* **1974**, *52*, 1006. (b) Back, R. A.; Willis, C. *Can. J. Chem.* **1974**, *52*, 2513. (c) Back, R. A.; Willis, C.; Ramsay, D. A. *Can. J. Chem.* **1978**, *56*, 1575. (d) Neudorfl, P. S.; Back, R. A.; Douglas, A. E. *Can. J. Chem.* **1981**, *59*, 506.

(19) (a) Warshel, A.; Karplus, M. *J. Am. Chem. Soc.* **1974**, *96*, 5677. (b) Warshel, A. *Ann. Rev. Biophys. Bioeng.* **1977**, *6*, 273.

(20) (a) Rebane, K. K.; Rebane, T. K. *Izv. Akad. Nauk Est. SSR, Ser. Fiz.-Mat. i Tekh. Nauk* **1963**, *12*, 227. (b) Preem, R. A. *Tr. Inst. Fiz. i Astron., Akad. Nauk Est. SSR* **1963**, *20*, 114 and **1964**, *25*, 47. (c) Tang, J.; Albrecht, A. C. In *Raman Spectroscopy;* Szymanski, H. A., Ed.; Plenum Press: 1970; Vol. 2.

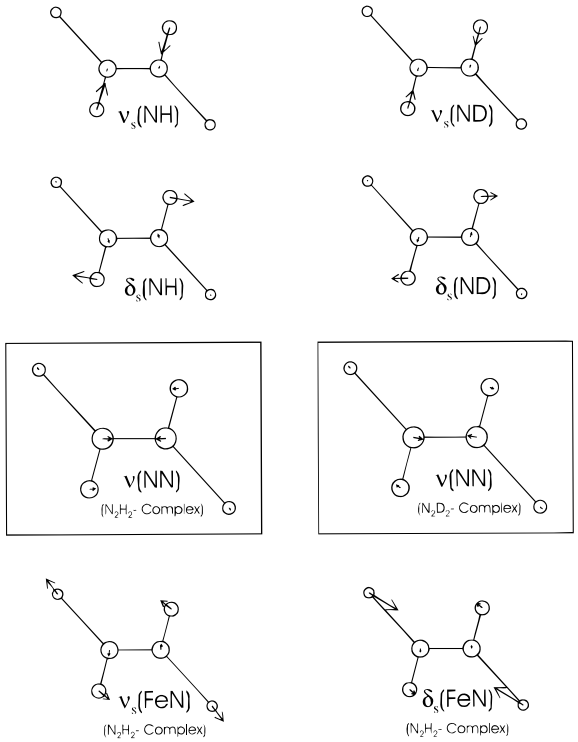

Figure 7. Eigenvectors for selected modes of the Fe-N_2H_2-Fe model. The arrows correspond to unit displacements of normal coordinates using a scaling factor of 10 for Fe displacements.

bond, increase of the NNH-angle and out-of-plane motion of the H atoms, the Fe−N bond distance should increase in the MLCT transition as the π^*_v orbital is Fe−N antibonding, whereas the transition originates from an orbital that is almost Fe−N nonbonding. According to the normal coordinate analysis, the symmetric Fe−N stretch should be very sensitive to isotope substitution and shift by 30 cm^{-1} upon deuteration. Nevertheless, no such peaks are detectable in the Raman spectra and one must conclude that the symmetric Fe−N stretch is not resonance enhanced with respect to the $d_{yz-}\pi_v \rightarrow \pi_v^*{}_-d_{yz}$ CT transition. This parallels the behavior of the symmetric metal−O stretches in cobalt[21] and copper[22] trans-μ-1,2 peroxo compounds. The observation that no enhancement occurs for the π^*_σ to metal(d_σ) transition has been explained by the fact that the electronic excitation from π^*_σ is delocalized over both halves of the dimer.[22] Hence, cancellation of the two individual metal−O stretching forces occurs leading to a vanishing displacement along the symmetric metal−O coordinate in the CT excited state. We assume that an equal explanation applies to the absence of resonance enhancement for the symmetric Fe−N stretch with respect to the $d_{yz-}\pi_v \rightarrow \pi_v^*{}_-d_{yz}$ MLCT transition in the Fe(II)-diazene systems: since the MLCT excited state is delocalized over the entire dimer, no enhancement of the symmetric Fe−N stretch is observed.

Finally, the bending mode δ_s(FeN) cannot be identified in the resonance Raman spectra of I and II. According to the NCA, the symmetric Fe−N-bending vibration shows only very small shifts on isotopic substitution with ^2H or ^{15}N. Therefore, one of the peaks around 350 or 310 cm^{-1} of compound II possibly belongs to this mode, but without isotopic shift an unambiguous assignment cannot be made.

In summary, the MLCT-excited state distortion emerging from the Raman enhancements certainly involves an elongation of the N−N bond, some out-of-plane bending motion of the diazene hydrogen atoms and probably some enlargement of the in-plane NNH-angle. Unfortunately, these structural changes do not offer clear insight in the nature of the photoexcited state involved in the presumed photoisomerization upon laser irradiation (see resonance Raman measurements). For the transition state involved in the thermal isomerization of compound I, Sellmann has proposed a linear end-on bridging N_2 unit with π-bonded hydrogen atoms.[2] Since the MLCT transition does not involve any weakening of the N−H bonds, the MLCT state certainly does not bear any direct connection to the linear N_2-bridged structure. Of course, this transition state at some hundred wavenumbers above the ground state could be populated after radiationless deactivation of the MLCT state. Alternatively, the hydrogen atoms remain σ-bound to the N_2 moiety after primary excitation, and the transition state involves a side-on bridging diazene (or diazenido(−)) group.[23] Without further information, this question cannot be decided at present.

C. Conclusions. 1. The vibrational frequencies and force constants of the Fe(II)−diazene unit are consistent with a σ-donor π-acceptor bond of diazene to the iron−sulfur centers. With an N−N force constant of 7.7 mdyn/Å, diazene is about halfway activated to the hydrazido(2−) level (bond order 1.6). No major change in N−H bonding is observed upon complexation. The Fe(II)−N(diazene) force constant of 1.8 mdyn/Å is 2.5 times as large as for a Fe(II)−N single bond.

2. The resonance Raman spectra can be understood on the basis of the assignment of the 580 and 620 nm bands of complex I and II, respectively, as metal-to-ligand charge transfer (MLCT) transitions into the diazene-type LUMO. This low-lying π^*_v orbital is central to the further reduction of diazene to hydrazine. The excited-state distortion primarily consists of an elongation of the N−N bond, with some contribution of in-plane and out-of-plane N−H-bending motions. Obviously no displacement occurs along the symmetric Fe−N- and N−H-stretching motions.

3. The doubling of N−H and N−D vibrations observed in the Raman but not in the IR spectra of compound II is attributed to a photoisomerization process upon laser irradiation into the π^*_v orbital of diazene. There is no direct connection between this process and the linear N_2-bridged transition state proposed for thermal isomerization since the MLCT state is not dissociative with respect to the N−H bonds of diazene.

Acknowledgment. F.T. gratefully acknowledges the support of these investigations by the Deutsche Forschungsgemeinschaft (Grant Tu58/4-1 and Tu58/5-1) and thanks Dr. J.-F. Létard for recording the excitation profiles of compound II. N.L. thanks the Fonds der Chemischen Industrie for a Kekulé Research Fellowship. We thank Dr. T. Schönherr and R. Linder, Institut für Theoretische Chemie at the Heinrich-Heine-Universität Düsseldorf, for the opportunity to record the low-temperature IR spectra and their support during the measurements.

JA970420X

(21) Tuczek, F.; Solomon, E. I. *Inorg. Chem.* **1992**, *31*, 944.
(22) Baldwin, M. J.; Ross, P. K.; Pate, J. E.; Tyeklar, Z.; Karlin, K. D.; Solomon, E. I. *J. Am. Chem. Soc.* **1991**, *113*, 8671.
(23) (a) Blum, L.; Williams, I. D.; Schrock, R. R. *J. Am. Chem. Soc.* **1984**, *106*, 8317. (b) Schrock, R. R.; Glassman, T. E.; Vale, M. G.; Kol, M. *J. Am. Chem. Soc.* **1993**, *115*, 1760.